PROCEEDINGS OF SCIENCE

Global Analyses of Polarized DIS & SIDIS from Small-x Evolution

Matthew D. Sievert[a,*] **and Nicholas Baldonado**[a]

[a] *Department of Physics, New Mexico State University, Las Cruces, New Mexico, 88003, USA*

E-mail: msievert@nmsu.edu, nbaldona@nmsu.edu

Quantifying the spin structure of the proton in terms of its quark and gluon constituents has been an animating goal of high-energy nuclear physics for decades. But a full understanding of the proton spin structure will necessarily require an extrapolation to small x, beyond measured data, where theoretical guidance is essential. In this work, we summarize recent developments in the theory and phenomenology of spin at small x, presenting results of a recent global analysis of inclusive and semi-inclusive deep inelastic scattering.

25th International Spin Physics Symposium (SPIN 2023)
24-29 September 2023
Durham, NC, USA

*Speaker

PoS(SPIN2023)185

1. Introduction

For forty years, an understanding of how the proton spin emerges from its quark and gluon substructure [1]

$$S_q + L_q + S_G + L_G = \frac{1}{2} \tag{1}$$

has remained elusive [2, 3]. In contrast to the naive expectation of quark spin pairing in an s-wave ground state, the measured contribution S_q from quark polarization is small, of order 25% of the proton spin. The revelation that there is substantial gluon polarization S_G and room for orbital angular momentum of L_q quarks and L_G of gluons underscores the tremendous differences in bound-state structure between quantum electrodynamics (QED) and quantum chromodynamics (QCD).

The quark S_q and gluon S_G spin contributions are obtained from integrals over the helicity parton distribution functions (hPDFs),

$$S_q(Q^2) = \frac{1}{2}\int_0^1 dx\, \Delta\Sigma(x,Q^2) = \frac{1}{2}\sum_f \int_0^1 dx\, \Delta q_f^+(x,Q^2) \tag{2a}$$

$$S_G(Q^2) = \int_0^1 dx\, \Delta G(x,Q^2)\,, \tag{2b}$$

where $\Delta q_f^+ = \Delta q_f + \Delta\bar{q}_f$ is the density of polarized quarks (plus antiquarks) of flavor f and ΔG is the density of polarized gluons. As clearly shown in Eqs. (2), the calculation of the proton spin contributions requires integration over the *full physical range* of $0 \le x \le 1$, while any experimental extraction of the hPDFs is kinematically limited to finite $x_{min} \propto 1/\sqrt{s} > 0$ by the finite collision energy $\sqrt{s}$. As such, the extrapolation beyond measured data to asymptotically small x is always a necessary feature of an analysis of the proton spin.

In traditional methods of extracting hPDFs (see, e.g. [4, 5]) based on collinear factorization and Dokshitzer-Gribov-Lipatov-Altarelli-Parisi (DGLAP) evolution [6, 7] , this indeed occurs as a pure extrapolation of the functional form obtained at larger x. But, in recent years, a new framework based on the theory of QCD at small x has emerged which makes first-principles predictions about the small-x tails of hPDFs. The first small-x analysis of hPDFs by Bartels, Ermolaev, and Ryskin (BER) [8, 9] used the method of "infrared evolution equations" [10, 11] which are structurally similar to the DGLAP evolution equations. This formalism has been used in various phenomenological applications [12, 13].

Since then, an s-channel formalism has been constructed which generalizes the methods of eikonal Wilson lines and impact factors at small x to include sub-eikonal and spin-dependent interactions. Spin-dependent small-x evolution equations (herein referred to as "KPS evolution") using polarized dipole amplitudes were first derived in Ref. [14]. Initially formulated only for flavor-singlet observables in terms of the forward S-matrix of a polarized dipole, KPS evolution was used to study flavor non-singlet observables [15] and reformulated at the operator level [16]. Crucially, the KPS evolution equations were constructed by keeping only the helicity-dependent terms of the sub-eikonal Wilson line interactions. While keeping only spin-dependent terms to

describe a spin-dependent observable seemed like a safe assumption at the time, in truth the KPS evolution equations missed an important *unpolarized* sub-eikonal contribution. Sub-eikonal recoil corrections, while spin independent, nevertheless contribute to the helicity evolution equations by diluting the azimuthal correlations generated by other, spin-dependent interactions. This fact was recognized in Ref. [17], which computed the new recoil operators and updated the small-x helicity evolution equations (hereafter: "KPS-CTT evolution").

The impact of KPS(-CTT) evolution on the hPDFs has been studied in a series of increasingly sophisticated analyses. For KPS evolution, the asymptotic power-law scaling of the hPDFs

$$\Delta\Sigma(x,Q^2) \sim \Delta G(x,Q^2) \sim \left(\frac{1}{x}\right)^{\alpha_h} , \tag{3}$$

was computed numerically in Ref. [18] and analytically in Ref. [19], obtaining an intercept value of $\alpha_h^{(KPS)} = \frac{4}{\sqrt{3}}\sqrt{\frac{\alpha_s N_c}{2\pi}} \approx 2.31\sqrt{\frac{\alpha_s N_c}{2\pi}}$ in the large-N_c limit. With the inclusion of the CTT recoil terms, the large-N_c intercept increases to $\alpha_h^{(KPS-CTT)} \approx 3.66\sqrt{\frac{\alpha_s N_c}{2\pi}}$ [17, 20], bringing it into quantitative agreement with the large-N_c intercept obtained by BER [8, 9]. Interestingly, a small numerical discrepancy remains between the KPS-CTT and BER intercepts in the large-$N_c\&N_f$ limit at the few percent level [21] which merits further investigation.

Phenomenologically, the early works based on KPS(-CTT) evolution did not attempt a global analysis; they simply explored the possible impact on S_g, S_Q by discontinuously switching from an existing, DGLAP-based global analysis to the asymptotic behavior (3). These results suggested that the impact from polarized small-x evolution could lead to significant enhancements in the total proton spin contributions S_g, S_Q. A first true global analysis based on KPS evolution was implemented in Ref. [22], which analyzed inclusive deep inelastic scattering (DIS). While the available dataset for DIS at small x was limited ($N_{pts} = 122$), this analysis was remarkable in that it successfully described the world DIS data using the small-x dipole formalism rather than a DGLAP-based analysis. Encouragingly, when extrapolated beyond the reach of the dataset, the uncertainty in the KPS predictions for the g_1 structure function at small x remained controlled, while the uncertainty from DGLAP-based, pure extrapolation methods grew substantially once the available data constraints ran out. This analysis seemed to substantiate the premise of the small-x theoretical formalism: by using first-principles input from the theory of spin at small x, a significant improvement in the uncertainty in S_q, S_G from small x can be achieved.

The most recent such global analysis was conducted in Ref. [23], which studied both inclusive DIS and semi-inclusive DIS (SIDIS) using the full KPS-CTT evolution equations in the more precise large-$N_c\&N_f$ limit. A summary of the methods and findings of that analysis is the subject of the remainder of this paper. Please see the full text of Ref. [23] for details that are beyond the scope of this paper.

2. Global Analysis of DIS + SIDIS

In the KPS(-CTT) formalism, the hPDFs are expressed in terms of *polarized dipole amplitudes*, Q_f for quarks of a given flavor, and G_2 for gluons. These dipole amplitudes are functions of a transverse size like x_{10} and a longitudinal momentum fraction z, and they contribute to the quark

hPDFs Δq_f^+, gluon hPDF ΔG, and helicity structure function g_1 according to

$$g_1(x,Q^2) = \frac{1}{2}\sum_f e_f^2\,\Delta q_f^+(x,Q^2)\,, \tag{4a}$$

$$\Delta q^+(x,Q^2) = -\frac{N_c}{2\pi^3}\int\limits_{\Lambda^2/s}^{1}\frac{dz}{z}\int\limits_{1/zs}^{\min\left[1/zQ^2,1/\Lambda^2\right]}\frac{dx_{10}^2}{x_{10}^2}\,\left[Q_q(x_{10}^2,zs)+2\,G_2(x_{10}^2,zs)\right]\,, \tag{4b}$$

$$\Delta G(x,Q^2) = \frac{2N_c}{\alpha_s\pi^2}\,G_2\!\left(x_{10}^2=\frac{1}{Q^2},zs=\frac{Q^2}{x}\right)\,. \tag{4c}$$

It is the polarized dipole amplitudes that evolve in x, resumming double logarithms of the form $\alpha_s\ln^2\frac{1}{x}$. The resulting KPS-CTT evolution equations, in the large-$N_c\&N_f$ limit, are

$$\begin{aligned}Q_f(x_{10}^2,zs) &= Q_f^{(0)}(x_{10}^2,zs) + \frac{N_c}{2\pi}\int_{1/x_{10}^2 s}^{z}\frac{dz'}{z'}\int_{1/z's}^{x_{10}^2}\frac{dx_{21}^2}{x_{21}^2}\,\alpha_s\!\left(\tfrac{1}{x_{21}^2}\right)\,\Big[2\,\widetilde{G}(x_{21}^2,z's)+2\,\widetilde{\Gamma}(x_{10}^2,x_{21}^2,z's)\\ &\quad + Q_f(x_{21}^2,z's) - \overline{\Gamma}_f(x_{10}^2,x_{21}^2,z's) + 2\,\Gamma_2(x_{10}^2,x_{21}^2,z's) + 2\,G_2(x_{21}^2,z's)\Big]\\ &\quad + \frac{N_c}{4\pi}\int_{\Lambda^2/s}^{z}\frac{dz'}{z'}\int\limits_{1/z's}^{\min\left[x_{10}^2 z/z',1/\Lambda^2\right]}\frac{dx_{21}^2}{x_{21}^2}\,\alpha_s\!\left(\tfrac{1}{x_{21}^2}\right)\,\left[Q_f(x_{21}^2,z's)+2\,G_2(x_{21}^2,z's)\right]\,,\end{aligned} \tag{5a}$$

$$\begin{aligned}G_2(x_{10}^2,zs) &= G_2^{(0)}(x_{10}^2,zs)\\ &\quad + \frac{N_c}{\pi}\int\limits_{\Lambda^2/s}^{z}\frac{dz'}{z'}\int\limits_{\max\left[x_{10}^2,\frac{1}{z's}\right]}^{\min\left[\frac{z}{z'}x_{10}^2,\frac{1}{\Lambda^2}\right]}\frac{dx_{21}^2}{x_{21}^2}\,\alpha_s\!\left(\tfrac{1}{x_{21}^2}\right)\,\left[\widetilde{G}(x_{21}^2,z's)+2\,G_2(x_{21}^2,z's)\right]\,,\end{aligned} \tag{5b}$$

$$\begin{aligned}\widetilde{G}(x_{10}^2,zs) &= \widetilde{G}^{(0)}(x_{10}^2,zs) + \frac{N_c}{2\pi}\int_{1/x_{10}^2 s}^{z}\frac{dz'}{z'}\int_{1/z's}^{x_{10}^2}\frac{dx_{21}^2}{x_{21}^2}\,\alpha_s\!\left(\tfrac{1}{x_{21}^2}\right)\,\Big[3\,\widetilde{G}(x_{21}^2,z's)+\widetilde{\Gamma}(x_{10}^2,x_{21}^2,z's)\\ &\quad + 2\,G_2(x_{21}^2,z's) + \left(2-\frac{N_f}{2N_c}\right)\Gamma_2(x_{10}^2,x_{21}^2,z's) - \frac{1}{4N_c}\sum_f\overline{\Gamma}_f(x_{10}^2,x_{21}^2,z's)\Big]\\ &\quad - \frac{1}{8\pi}\int_{\Lambda^2/s}^{z}\frac{dz'}{z'}\int\limits_{\max[x_{10}^2,\,1/z's]}^{\min\left[x_{10}^2 z/z',1/\Lambda^2\right]}\frac{dx_{21}^2}{x_{21}^2}\,\alpha_s\!\left(\tfrac{1}{x_{21}^2}\right)\,\left[\sum_f Q_f(x_{21}^2,z's)+2\,N_f\,G_2(x_{21}^2,z's)\right]\,.\end{aligned} \tag{5c}$$

The quark dipole Q_f and gluon dipole G_2 mix with a third amplitude $\widetilde{G}$ under evolution, and for each of the three dipole amplitudes $Q_f, G_2, \widetilde{G}$, there exists an equivalent auxiliary amplitude $\bar{\Gamma}_f, \Gamma_2, \widetilde{\Gamma}$ with modified limits of integration due to their dependence on the "neighbor dipole." We omit the analogous evolution equations of the auxiliary functions for brevity.

To study the proton helicity structure at small x, we solve Eqs. (5) numerically by discretizing the integral equations and solving them recursively. In doing so, it is convenient to change to the

logarithmic variables $s_{10} = \sqrt{\frac{N_c}{2\pi}} \ln \frac{1}{x_{10}^2 \Lambda^2}$ and $\eta = \sqrt{\frac{N_c}{2\pi}} \ln \frac{zs}{\Lambda^2}$. Because the evolution equations (5) are linear, if the large-x initial conditions are specified as a sum of terms, each of those terms evolves independently. This greatly facilitates the global analysis, permitting an expansion of the initial conditions in terms of a finite set of basis functions,

$$Q_f^{(0)} = a_f \, \eta + b_f \, s_{10} + c_f \,, \tag{6a}$$

$$\widetilde{G}^{(0)} = \widetilde{a} \, \eta + \widetilde{b} \, s_{10} + \widetilde{c} \,, \tag{6b}$$

$$G_2^{(0)} = a_2 \, \eta + b_2 \, s_{10} + c_2 \,, \tag{6c}$$

[4, 24]).

The observables we consider are the longitudinal double-spin asymmetries A_1 and $A_\parallel \propto A_1$ for DIS at SLAC, EMC, SMC, COMPASS, and HERMES, and A_1^h for identified hadrons h in SIDIS at SMC, COMPASS, and HERMES (see [23] for details on the experimental data utilized). We impose the kinematic cuts $5 \times 10^{-3} < x < 0.1 \equiv x_0$ and $1.69 \text{ GeV}^2 < Q^2 < 10.4 \text{ GeV}^2$ on the data to select on the small-x regime. The upper limit $x_0 = 0.1$ for the double-logarithmic helicity evolution coincides with the onset of *single*-logarithmic unpolarized evolution around 0.01 preferred by phenomenology [25, 26]. For SIDIS we use the JAM fragmentation functions from Ref. [5]. We choose our IR cutoff to be $\Lambda = 1$ GeV. We do not place any explicit cuts on the hadron momentum fraction z in SIDIS. We fit the remaining 122 polarized DIS data points and 104 polarized SIDIS data points with an overall χ^2/N_{pts} of 1.03. The extracted hPDFs are shown in Fig. 1.

Fig 1 summarizes our main results. The C-even quark hPDFs Δq_f^+ (Fig 1: Left) are distinct from each other at large x due to constraints from data, with all hPDFs decreasing in magnitude at small x. The large-x flavor separation disappears at small x, resulting in error bands that span zero, allowing for flavor-specific spin contributions that could be positive, negative, or consistent with zero. Meanwhile ΔG appears to have the largest error band of all, both at large and small-x, and also spanning zero. The C-odd hPDFs Δq_f^- (Fig 1: Right) exhibit flavor-specific behavior across the whole range of x, with visible differences in the bands persisting even to small x. The C-odd hPDFs converge to zero more quickly than the C-even ones because of the smaller intercept [15].

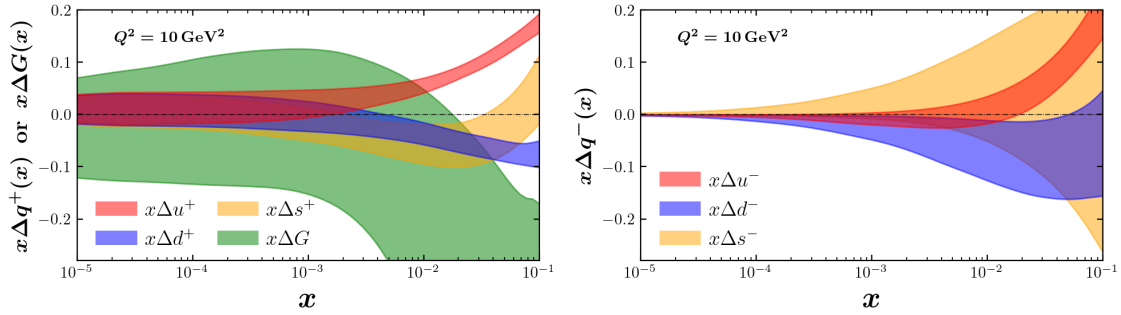

Figure 1: (Left) C-even quark hPDFs Δu^+ (red), Δd^+ (blue), Δs^+ (orange) and ΔG (green) extracted from experimental data and scaled by x. (Right) Extractions of the C-odd quark hPDFs Δu^- (red), Δd^- (blue), Δs^- (orange), also scaled by x.

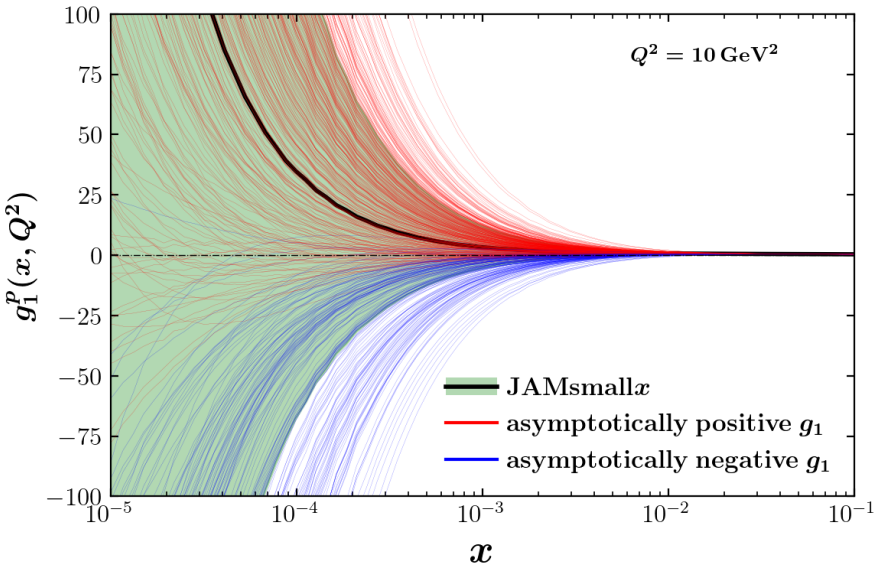

Figure 2: The small-x predictions of g_1^p. The black curve is the mean of all the replicas and the green band gives the 1σ uncertainty. Blue (red) curves are solutions that are asymptotically negative (positive).

In contrast to the precise predictions at small x obtained in Ref. [22], the hPDFs obtained in Fig. 1 exhibit surprisingly large uncertainties, precisely in the region where the theory should work best. To understand the origin of this large error, it is helpful to analyze the individual replicas generated by the global analysis depicted in Fig. 2. There we show 500 distinct replicas of g_1^p, each computed with a randomly-sampled set of initial-condition parameters. All replicas coincide in the region of x where we the data imposes constraints ($5 \times 10^{-3} < x < 0.1$), but the small-$x$ predictions begin to diverge from each other once the data runs out. The origin of the problem is clearly visible by eye (with the aid of the color coding in Fig. 2): small-x helicity evolution does indeed lead to the asymptotic power-law scaling (3) as expected, but the *sign* of that power-law behavior is not constrained from the fit to data.

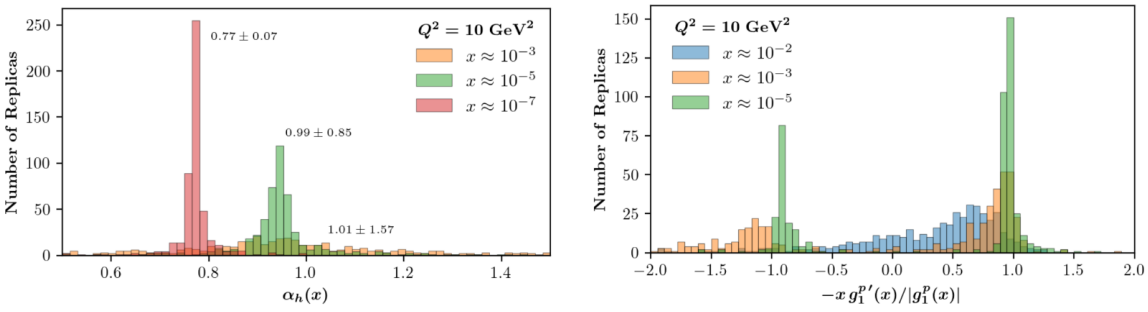

Figure 3: (Left) Histograms utilizing Eq. (7) showing that the intercept $\alpha_h(x)$ becomes more refined as x decreases. (Right) Keeping only the information on the sign dependence from the first derivative produces bimodal peaks at $\pm\alpha_h(x)$. At large x there is no asymptotic behavior, while two refined peaks emerge as the asymptotics take form at smaller values of x.

This picture can be further substantiated by studying the logarithmic derivative of the dipole amplitudes

$$\lim_{x\to 0} g_1^p(x) \equiv g_1^{p\,(0)}\, x^{-\alpha_h(x)} \qquad \therefore \qquad \alpha_h(x) \equiv \frac{1}{g_1^p(x)} \frac{d\, g_1^p(x)}{d\ln(1/x)}, \tag{7}$$

shown in Fig. 3 which provides a local, x-dependent measure of the power law $\alpha_h(x)$. The usual logarithmic derivative (Fig. 3: left) shows that the hPDFs all converge toward the asymptotic intercept α_h as $x \to 0$, but the signed logarithmic derivative (Fig. 3: left) reveals something more interesting. As the replicas evolve toward lower x, the distribution forms two bimodal clusters around $\pm\alpha_h(x)$. While quantum evolution consistently drives the *curvature* of each replica towards its asymptotic behavior (3), the *sign of the coefficient in front* must be fixed from fitting to the data. This is the origin of the increased uncertainty at small x in our analysis: not a failure of the small-x formalism itself, but an inability to sufficiently constrain all the coefficients within the current scope. As we demonstrate in Fig. 4, the inclusion of a small amount of additional constraining power (here, lower-x DIS pseudodata from the EIC) can resolve the ambiguity seen in Fig. 3 and restore precise predictive power to the global analysis.

An analysis of the structure of the hPDF basis functions [23] reveals which dipole amplitudes carry this uncertainty. The Q_f and G_2 polarized dipole amplitudes have relatively large magnitudes at large values of x and are therefore well-constrained by the experimental data. The evolution-only amplitude $\widetilde{G}$, however, is negligible in the large-x region and only becomes non-zero for small values of x. Because of this, $\widetilde{G}$ is poorly constrained from the fit to data, and the large uncertainty at small x can be attributed to the unconstrained sign of $\widetilde{G}$. Since the quark and gluon hPDFs mix under evolution, any unconstrained parameters in $\widetilde{G}$ will strongly influence the uncertainty in the other hPDFs.

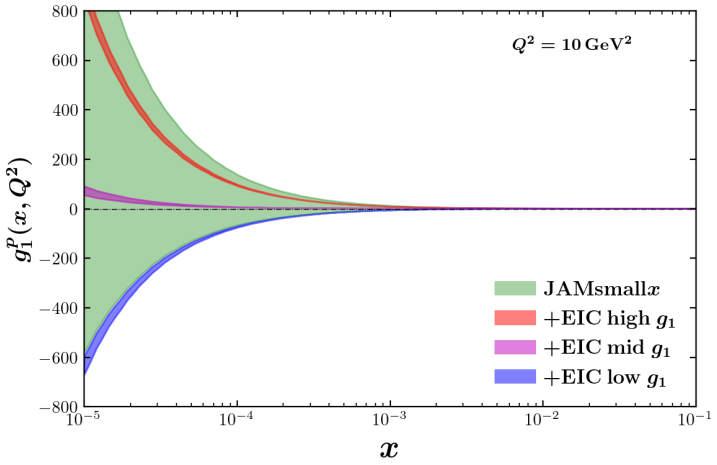

Figure 4: Impact on the current fit to the proton structure function g_1^p (green, same as Fig. 2) from EIC pseudodata under three scenarios of "high" (red), "mid" (magenta), and "low" (blue) values.

3. Outlook

Our future work will be dedicated to obtaining better constraints on our initial condition parameters, with emphasis on the amplitudes $\widetilde{G}$ and G_2 which are dominant at small x. One strategy we are exploring is to perform matching onto the well-developed predictions of the collinear factorization formalism (e.g. [4, 24, 27]) in the neighborhood of $x \approx 0.1$. A first attmept at large-x matching was performed in [23], and the results indicated that even a rudimentary matching procedure can substantially change the fit. More realistic matching procedures that guarantee smoothness at the matching point would allow for a continuous fit valid over all values of x, which we are pursuing for future work.

Another possible strategy to resolve the present ambiguity would be to expand the scope of the global analysis to include new observables sensitive to the differences between the basis functions. To have the greatest impact on the small-x uncertainty, these observables should specifically couple to the gluon-dominated dipoles $\widetilde{G}$ and G_2. For these reasons, it is very promising to pursue the implementation of the longitudinal double spin asymmetry A_{LL} of hadrons and jets produced at mid-rapidity in pp collisions. Adding this observable not only increases the number of data points, but also adds sensitivity to the gluon hPDF at leading order.

The theory and phenomenology of spin at small x is a rapidly developing field, with its importance to resolving the proton spin puzzle becoming increasingly clear. Significant progress is expected on these fronts in the coming years through the activities of the SURGE Collaboration, which seeks to provide the framework for a comprehensive global analysis of polarized and unpolarized reactions in the small-x regime. Taken together, the polarized and unpolarized components of the SURGE Collaboration's efforts will make important contributions not only to the study of the proton spin, but also to the search for gluon saturation as well.

Acknowledgments

M.S. is supported by the U.S. Department of Energy, Office of Science through the FAIR program under Award Number DE-SC0024560. This work is also supported by the U.S. Department of Energy, Office of Science, Office of Nuclear Physics, within the framework of the Saturated Glue (SURGE) Topical Theory Collaboration.

References

[1] R. L. Jaffe and A. Manohar, *The G(1) Problem: Fact and Fantasy on the Spin of the Proton*, *Nucl. Phys.* **B337** (1990) 509–546.

[2] C. A. Aidala, S. D. Bass, D. Hasch and G. K. Mallot, *The Spin Structure of the Nucleon*, *Rev. Mod. Phys.* **85** (2013) 655–691, [1209.2803].

[3] E. Leader and C. Lorcé, *The angular momentum controversy: What's it all about and does it matter?*, *Phys. Rept.* **541** (2014) 163–248, [1309.4235].

[4] JAM Collaboration collaboration, E. Moffat, W. Melnitchouk, T. C. Rogers and N. Sato, *Simultaneous Monte Carlo analysis of parton densities and fragmentation functions*, *Phys. Rev. D* **104** (2021) 016015, [2101.04664].

[5] JAM Collaboration collaboration, C. Cocuzza, W. Melnitchouk, A. Metz and N. Sato, *Polarized antimatter in the proton from a global QCD analysis*, *Phys. Rev. D* **106** (2022) L031502, [2202.03372].

[6] V. N. Gribov and L. N. Lipatov, *Deep inelastic e p scattering in perturbation theory*, *Sov. J. Nucl. Phys.* **15** (1972) 438–450.

[7] G. Altarelli and G. Parisi, *Asymptotic Freedom in Parton Language*, *Nucl. Phys.* **B126** (1977) 298.

[8] J. Bartels, B. I. Ermolaev and M. G. Ryskin, *Nonsinglet contributions to the structure function g1 at small x*, *Z. Phys. C* **70** (1996) 273–280, [hep-ph/9507271].

[9] J. Bartels, B. Ermolaev and M. Ryskin, *Flavor singlet contribution to the structure function G(1) at small x*, *Z. Phys. C* **72** (1996) 627–635, [hep-ph/9603204].

[10] V. G. Gorshkov, V. N. Gribov, L. N. Lipatov and G. V. Frolov, *Doubly logarithmic asymptotic behavior in quantum electrodynamics*, *Sov. J. Nucl. Phys.* **6** (1968) 95.

[11] R. Kirschner and L. Lipatov, *Double Logarithmic Asymptotics and Regge Singularities of Quark Amplitudes with Flavor Exchange*, *Nucl. Phys.* **B213** (1983) 122–148.

[12] B. I. Ermolaev, M. Greco and S. I. Troyan, *Running coupling effects for the singlet structure function g_1 at small x*, *Phys. Lett.* **B579** (2004) 321–330, [hep-ph/0307128].

[13] B. I. Ermolaev, M. Greco and S. I. Troyan, *Overview of the spin structure function g_1 at arbitrary x and Q^2*, *Riv. Nuovo Cim.* **33** (2010) 57–122, [0905.2841].

[14] Y. V. Kovchegov, D. Pitonyak and M. D. Sievert, *Helicity Evolution at Small-x*, *JHEP* **01** (2016) 072, [1511.06737].

[15] Y. V. Kovchegov, D. Pitonyak and M. D. Sievert, *Helicity Evolution at Small x: Flavor Singlet and Non-Singlet Observables*, *Phys. Rev. D* **95** (2017) 014033, [1610.06197].

[16] Y. V. Kovchegov and M. D. Sievert, *Small-x Helicity Evolution: an Operator Treatment*, *Phys. Rev. D* **99** (2019) 054032, [1808.09010].

[17] F. Cougoulic, Y. V. Kovchegov, A. Tarasov and Y. Tawabutr, *Quark and gluon helicity evolution at small x: revised and updated*, *JHEP* **07** (2022) 095, [2204.11898].

[18] Y. V. Kovchegov, D. Pitonyak and M. D. Sievert, *Small-x asymptotics of the quark helicity distribution*, *Phys. Rev. Lett.* **118** (2017) 052001, [1610.06188].

[19] Y. V. Kovchegov, D. Pitonyak and M. D. Sievert, *Small-x Asymptotics of the Quark Helicity Distribution: Analytic Results*, *Phys. Lett. B* **772** (2017) 136–140, [1703.05809].

[20] J. Borden and Y. V. Kovchegov, *Analytic solution for the revised helicity evolution at small x and large Nc: New resummed gluon-gluon polarized anomalous dimension and intercept*, *Phys. Rev. D* **108** (2023) 014001, [2304.06161].

[21] D. Adamiak, Y. V. Kovchegov and Y. Tawabutr, *Helicity Evolution at Small x: Revised Asymptotic Results at Large N_c&N_f*, 2306.01651.

[22] JAM Collaboration collaboration, D. Adamiak, Y. V. Kovchegov, W. Melnitchouk, D. Pitonyak, N. Sato and M. D. Sievert, *First analysis of world polarized DIS data with small-x helicity evolution*, *Phys. Rev. D* **104** (2021) L031501, [2102.06159].

[23] Jefferson Lab Angular Momentum (JAM) collaboration, D. Adamiak, N. Baldonado, Y. V. Kovchegov, W. Melnitchouk, D. Pitonyak, N. Sato et al., *Global analysis of polarized DIS and SIDIS data with improved small-x helicity evolution*, *Phys. Rev. D* **108** (2023) 114007, [2308.07461].

[24] JAM Collaboration collaboration, N. Sato, C. Andres, J. J. Ethier and W. Melnitchouk, *Strange quark suppression from a simultaneous Monte Carlo analysis of parton distributions and fragmentation functions*, *Phys. Rev. D* **101** (2020) 074020, [1905.03788].

[25] J. L. Albacete, N. Armesto, J. G. Milhano and C. A. Salgado, *Non-linear QCD meets data: A Global analysis of lepton-proton scattering with running coupling BK evolution*, *Phys. Rev. D* **80** (2009) 034031, [0902.1112].

[26] J. L. Albacete, N. Armesto, J. G. Milhano, P. Quiroga-Arias and C. A. Salgado, *AAMQS: A non-linear QCD analysis of new HERA data at small-x including heavy quarks*, *Eur. Phys. J. C* **71** (2011) 1705, [1012.4408].

[27] JAM Collaboration collaboration, N. Sato, W. Melnitchouk, S. Kuhn, J. Ethier and A. Accardi, *Iterative Monte Carlo analysis of spin-dependent parton distributions*, *Phys. Rev. D* **93** (2016) 074005, [1601.07782].

PoS(SPIN2023)185